

Structural Dynamics of Nucleosome Core Particle: Comparison with Nucleosomes Containing Histone Variants

Amutha Ramaswamy,¹ Ivet Bahar,² and Ilya Ioshikhes^{1*}

¹Department of Biomedical Informatics, The Ohio State University, Columbus, Ohio

²Center for Computational Biology and Bioinformatics, Department of Molecular Genetics and Biochemistry, School of Medicine, University of Pittsburgh, Pittsburgh, Pennsylvania

ABSTRACT The present study provides insights on the dominant mechanisms of motions of the nucleosome core particle and the changes in its functional dynamics in response to histone variants. Comparative analysis of the global dynamics of nucleosomes with native and variant H2A histones, using normal mode analysis revealed that the dynamics of the nucleosome is highly symmetric, and its interaction with the nucleosomal DNA plays a vital role in its regulation. The collective dynamics of nucleosomes are predicted to be dominated by two types of large-scale motions: (1) a global stretching–compression of nucleosome along the dyad axis by which the nucleosome undergoes a breathing motion with a massive distortion of nucleosomal DNA, modulated by histone–DNA interactions; and (2) the flipping (or bending) of both the sides of the nucleosome in an out-of-plane fashion with respect to the dyad axis, originated by the highly dynamic N-termini of H3 and (H2A.Z–H2B) dimer in agreement with the experimentally observed perturbed dynamics of the particular N-terminus under physiological conditions. In general, the nucleosomes with variant histones exhibit higher mobilities and weaker correlations between internal motions compared to the nucleosome containing ordinary histones. The differences are more pronounced at the L1 and L2 loops of the respective monomers H2B and H2A, and at the N-termini of the monomers H3 and H4, all of which closely interact with the wrapping DNA. *Proteins* 2005;58:683–696.

© 2004 Wiley-Liss, Inc.

Key words: nucleosome dynamics; normal mode analysis; DNA–protein interactions; equilibrium fluctuations

INTRODUCTION

Nucleosome, the structural unit of chromatin, plays a vital role in chromatin biology,^{1,2} and understanding the dynamics of nucleosome is of fundamental importance in improving our knowledge of gene regulation and DNA replication machinery. The mystery of nucleosome and the regulation of its biological function have been issues of intense investigation over years. The structure of histones, the organization of the nucleosome, and the mechanism of transcriptional regulation as a result of nucleosome repositioning have been reviewed in several pioneering stud-

ies.^{2–4} Stable alterations in nucleosome structure generate a transient state of chromatin as an essential step in gene regulation.⁴ Thus, the conformational dynamics of the nucleosome play a central role in determining the transcriptional competence of any region of the chromatin.

The structure of the nucleosome core particle was originally solved at 7 Å resolution in the early 1980s, and refined in later studies. Among these, the crystallographic structure at 2.8 Å resolution by Luger et al.⁵ in 1997 has revealed how the histone protein octamer is assembled, and how the 146 base pairs of DNA are organized into a superhelix around it. The nucleosome consists of 146 base pairs of DNA wrapped in a left-handed superhelix around an octameric histone core formed by 2 copies of each of the histone molecules H2A, H2B, H3, and H4.^{5,6} The (H3–H4)₂ tetramer occupies a central position in the octameric core structure, flanked on both sides by the (H2A–H2B) dimers,⁷ as can be viewed in Figure 1. The assembly of a stable nucleosome core depends on the initial heterodimerization of the H3 and H4 molecules, and their subsequent dimerization to form the (H3–H4)₂ tetramer,⁹ followed by the dimerization of the histones H2A and H2B that bind to both sides of the (H3–H4)₂ tetramer (Fig. 1).^{10,11} Changes in the accessibility of DNA to histones in response to environmental stimuli affect the mechanism of transcription and gene regulation.

The core histones share a structurally conserved motif called the histone fold and mobile extended regions at the chain termini (also named histone tails). The histone fold consists of 3 α -helices (α 1, α 2, and α 3) connected by short loops L1 and L2, respectively. During dimerization, loop L1 of one of the monomers (e.g., H3) aligns against loop L2 of the other monomer (e.g., H4) to form the so-called handshake motif (Fig. 2) that interacts with DNA. The flexible tails of the core histones interact with DNA via the minor groove. The histone tails are the major targets for post-translational modifications such as acetylation, methylation, and phosphorylation, and so are the key arbiters of

Grant sponsor: National Institutes of Health PRE-NPEBC; Grant number: 1 P20 GM065805-01A1 (to I. Bahar).

*Correspondence to: Ilya Ioshikhes, Department of Biomedical Informatics, Ohio State University, 3172c Graves Hall, 333 West Tenth Avenue, Columbus, OH 43210. E-mail: ioschikhes-1@medctr.osu.edu

Received 19 April 2004; Accepted 15 September 2004

Published online 28 December 2004 in Wiley InterScience (www.interscience.wiley.com). DOI: 10.1002/prot.20357

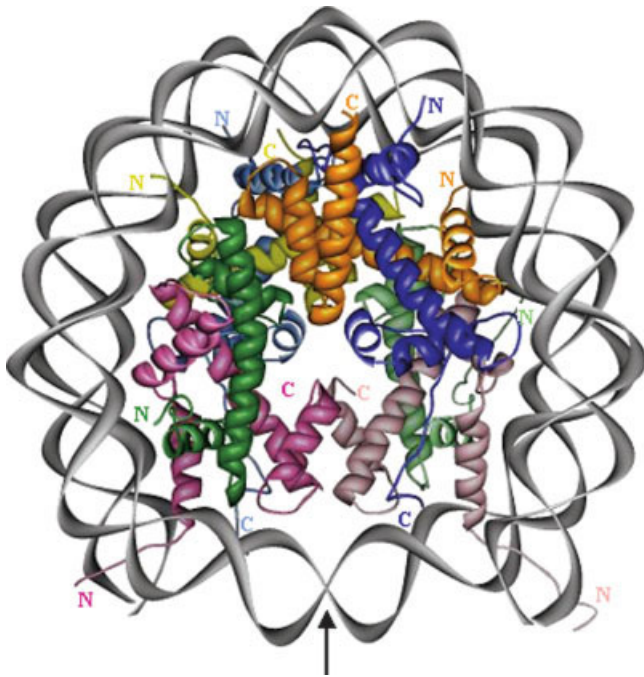


Fig. 1. Architecture of the octameric histones H3 (pink), H4 (green), H2A.Z (blue) and H2B (orange), and DNA (gray) in the nucleosome. Dark and light colors distinguish each copy of the monomers. The N- and C-termini are indicated. The arrow indicates the direction of the dyadic axis. The structure has been constructed using PDB file 1F66 for the nucleosome with the histone variant H2A.Z, deposited by Luger and coworkers.⁸

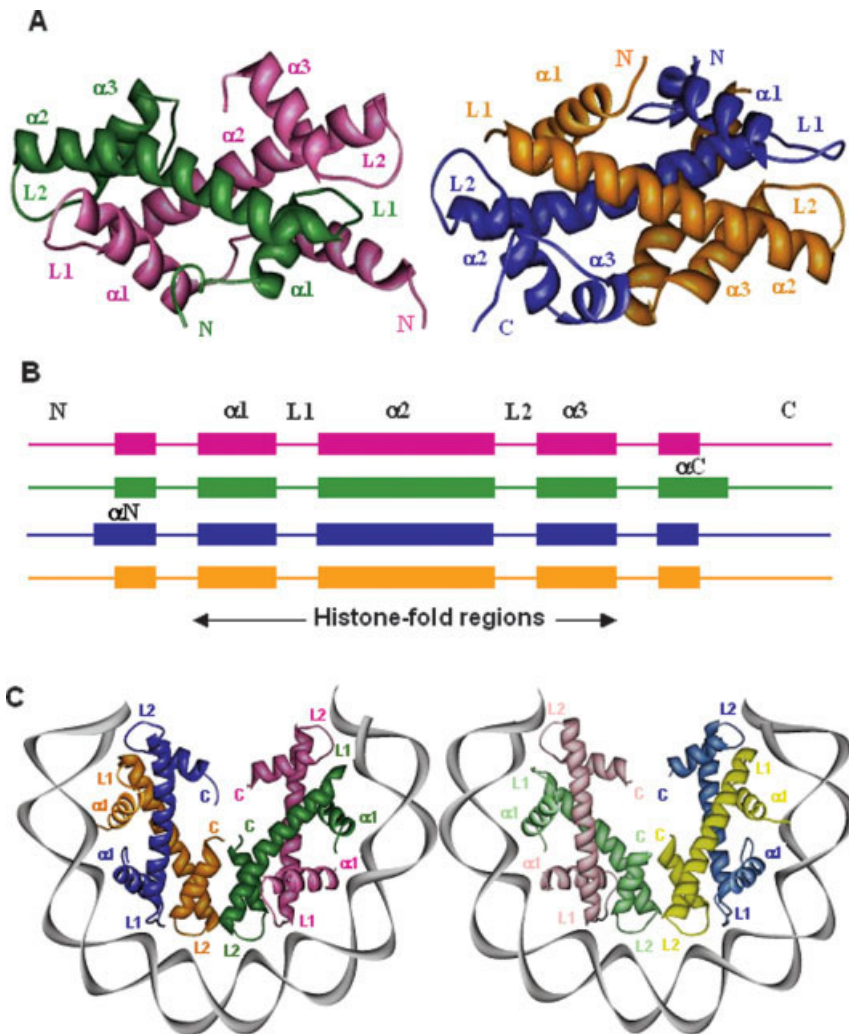


Fig. 2. (A) Handshake motifs formed by H3-H4 and H2A-H2B. The monomers H3, H4, H2Z, and H2B are colored pink, green, blue, and orange, respectively, consistent with Figure 1. (B) Schematic view of the secondary structure of the histones (colored as in A). (C) DNA-histone interaction sites (L1, L2 and $\alpha 1$, $\alpha 1$ sites), shown (after 180° rotation around the Z axis) separately for the 2 successive turns that enclose the successive copies of the 2 pairs of histone folds. The colors and labels are in accord with those used in Figure 1.

chromatin function.¹² The octameric histones and the DNA are highly networked by hydrogen bonds and the major DNA–protein interaction sites of the dimers are the 2 pairs of adjoining loops L1 and L2, and the $\alpha 1$ helices of the monomers [Fig. 2(C)].

Natural types of histones occur in the form of various isoforms (H2A.1, H2A.2), variants (H2A.Z, H2A.X, H3.3, and CENP-A), and histone-like proteins (macroH2A). *Drosophila* chromatin contains, for example, 2 H2A histones, H2A.1 and H2A.2, that differ in their amino acid compositions and their antigenically distinct functions. H2A.Z, a minor variant of H2A, is essential for the viability of many organisms and has functions distinct from those of the major H2A histone in chromatin. A number of recent studies have focused on the chromatin structures with variant histones given that the structure and function of the nucleosome are influenced by the core histone variants.

Several pioneering studies have reported the importance and the functional diversity of the nucleosome by H2A.Z.^{8,13–19} Activation of transcription within chromatin has been correlated with the incorporation of H2A.Z into the nucleosomes. Recently, a review article on the functional heterogeneity of the histone variants has been reported by Brown.¹³ H2A.Z is found in a wide range of organisms, from yeast to mammals.¹⁷ The elucidation of the H2A.Z nucleosome crystal structure has been instrumental in detecting the changes in the histone–DNA and histone–histone interactions within the nucleosome core containing histone variant⁸ compared to those in the major histone.

Having access to detailed sequence and structure information on the nucleosomes, it would be interesting to analyze the factors generating the distinct behavior of variant histones and hence the dynamics of nucleosome. Molecular simulation techniques using conventional full-atomic force fields^{20,21} are prohibitively time-consuming for exploring the dynamics of supramolecular structures like the nucleosome (which consists of $\sim 50,000$ atoms). On the other hand, normal modes analysis (NMA)^{22,23} proved to be an efficient but physically meaningful, complementary tool for analyzing the equilibrium dynamics of large structures and assemblies. Recently, simplified NMAs with uniform harmonic potentials, or methods based on elastic network formalism, have been proposed^{24–29} and successfully applied to several molecular systems.^{28–31} The Gaussian Network Model (GNM)^{25,26} and its extension, the Anisotropic Network Model (ANM),²⁹ introduced by Bahar and coworkers to predict the sizes or directionalities of residue motions in different modes, have been used advantageously in many applications.^{32–35} These models consider the biomolecule as an elastic network (EN) and generate a connectivity matrix by considering the C α atoms as nodes. The connectivity of the network is determined by defining an appropriate cutoff (r_c) distance for pairs of amino acids that interact via elastic springs. For proteins, the effective network is generated using $r_c \leq 10$ Å, whereas in DNA, as well as RNA, a slightly increased cutoff distance of $\sim 14 \pm 2$ Å has been used to include

interstrand interactions of DNA.^{36–38} The topology of the network is represented by a connectivity (Kirchhoff) matrix whose eigenvalue decomposition yields the normal modes of motion near the equilibrium structure. The GNM has proven to be a useful technique in predicting X-ray crystallographic B factors,²⁵ H/D exchange free energies near native state conditions,³⁰ and NMR order parameters.³¹ It has also been extensively used for identifying the cooperative domain motions that underlie biomolecular function.^{36,37,39–41}

In this work, the *global* dynamics of nucleosomes with variant histones are analyzed with the EN models and compared to highlight the effect of variant histones on the functional motions of the nucleosome. Global dynamics refer to the lowest frequency (and largest amplitude) modes of motions, which have been shown in several studies for other systems to be relevant to biological function.^{33–43} The analysis aims at answering a number of fundamental questions: What are the dominant molecular mechanisms that control the relaxation of the nucleosome? To what degree do the variant histones influence the dynamics and intradomain interactions of the nucleosome? What are the factors causing the divergent functions of histone variants?

METHODOLOGY

The structural dynamics of the nucleosome with regular histones,⁴⁴ nucleosome containing the variant histone H2A.Z,⁸ and the histone with isoforms H2A.1 and H2B.2⁴⁵ are analyzed to unravel the changes in the conformational motions of the different nucleosome structures. The respective crystal structures 1EQZ, 1F66, and 1KX4 were downloaded from the Protein Data Bank (PDB).⁴⁶ 1F66 corresponds to the recombinant mouse H2A.Z and recombinant *Xenopus laevis* H2B, H3, and H4. The nucleosome 1KX4 is of *X. laevis* origin, and 1EQZ refers to the chicken (*Gallus gallus*) histone octamer. Despite the differences in the originating organisms, the nucleosomes possess high (> 95%) sequence identity except for the variant histone H2A.Z. The alignment presented in Figure 3 shows that the histone molecules, H3 and H4, are sequentially identical in the 3 structures except for 1 residue in H3. H2A.1 sequence (PDB ID: 1KX4) is closely similar to H2A sequence (PDB ID: 1EQZ), and H2B.2 (in 1KX4) is identical to the H2B in *X. laevis*. Considerable variation in sequence is, however, observed between H2A (1EQZ) and H2A.Z variant (1F66). The structures also differ in their lengths (mainly histone tails): The crystal structure of 1F66 has 769 histone residues, and 1EQZ has 883 residues.

Despite the differences in sequence, the 3 structures are closely superimposable. The root-mean-square deviations (RMSDs) between α -carbon coordinates are 0.50 Å, 0.46 Å, and 0.56 Å for the respective pairs (1EQZ, 1F66), (1EQZ, 1KX4), and (1KX4, 1F66), and the corresponding RMSDs of all atoms including the respective DNA segments are 0.59 Å, 0.46 Å, and 0.56 Å. The interactions between H2A.Z and H2B are generally similar to those between H2A and H2B. On the other hand, localized changes exist in the interactions of H2A.Z–H2B dimer with the (H3–H4)₂

```

1EQZ:H3      KKPHRYRPGTVALREIRRYQKSTELLIRKLPFQRLVREIAQDFKTDLRFQSSAVMALQEA
1F66:H3      KKPHRYRPGTVALREIRRYQKSTELLIRKLPFQRLVREIAQDFKTDLRFQSSAVMALQEA
1KX4:H3      --PHRYRPGTVALREIRRYQKSTELLIRKLPFQRLVREIAQDFKTDLRFQSSAVMALQEA
1EQZ:H3      SEAYLVGLFEDTNLCAIHAKRVTIMPKDIQLARRIRGER
1F66:H3      SEAYLVGLFEDTNLCAIHAKRVTIMPKDIQLARRIRGER
1KX4:H3      SEAYLVGLFEDTNLCAIHAKRVTIMPKDIQLARRIRGER

1EQZ:H4      RDNIQGITKPAIRRLARRGGVKRISGLIYEETRGLVKVFLENVIRDAVTYTEHAKRKTVT
1F66:H4      RDNIQGITKPAIRRLARRGGVKRISGLIYEETRGLVKVFLENVIRDAVTYTEHAKRKTVT
1KX4:H4      -DNIQGITKPAIRRLARRGGVKRISGLIYEETRGLVKVFLENVIRDAVTYTEHAKRKTVT
1EQZ:H4      AMDVVYALKRQGRTLYGFGG
1F66:H4      AMDVVYALKRQGRTLYGFGG
1KX4:H4      AMDVVYALKRQGRTLYGFGG

1EQZ:H2A     AKSRSSRAGLQFPVGRVHRLLRKGNYA-ERVGAGAPVYLAAVLEYLTAELELAGNAARD
1F66:H2A.Z   AVSRSSRAGLQFPVGRVHRLLRKSRTTSHGRVGATAAVYSAALEYLTAELELAGNASKD
1KX4:H2A.1   --TRSSRAGLQFPVGRVHRLLRKGNYA-ERVGAGAPVYLAAVLEYLTAELELAGNAARD
1EQZ:H2A     NKKTRIPRHLQLAIRNDEELNLLKRTIAQGGVLPNIQAVLL
1F66:H2A.Z   LKVKRIPRHLQLAIRNDEELSLI-KATIAQGGVLPNIHKSLLI
1KX4:H2A.1   NKKTRIPRHLQLAIRNDEELNLLKGRVTIAQGGVLPNIQSVLL

1EQZ:H2B     SRKESYSIYVYKVLKQVHPDTGISSKAMIMNSFVNDVFERIAGEASRLAHYNKRSTITS
1F66:H2B     TRKESYAIYVYKVLKQVHPDTGISSKAMIMNSFVNDVFERIAGEASRLAHYNKRSTITS
1KX4:H2B.2   TRKESYAIYVYKVLKQVHPDTGISSKAMIMNSFVNDVFERIAGEASRLAHYNKRSTITS
1EQZ:H2B     REIQTAVRLLLPGELAKHAVSEGTKAVTKYTS
1F66:H2B     REIQTAVRLLLPGELAKHAVSEGTKAVTKYTS
1KX4:H2B.2   REIQTAVRLLLPGELAKHAVSEGTKAVTKYTS
    
```

Fig. 3. Comparison of the histone sequences of 1EQZ (major histone), 1F66 (histone with the H2A.Z variant), and 1KX4 (histone with the isoforms H2A.1 and H2B.2). The differences in the amino acid sequences of 1EQZ and 1F66 (and 1KX4) are highlighted in green (and yellow).

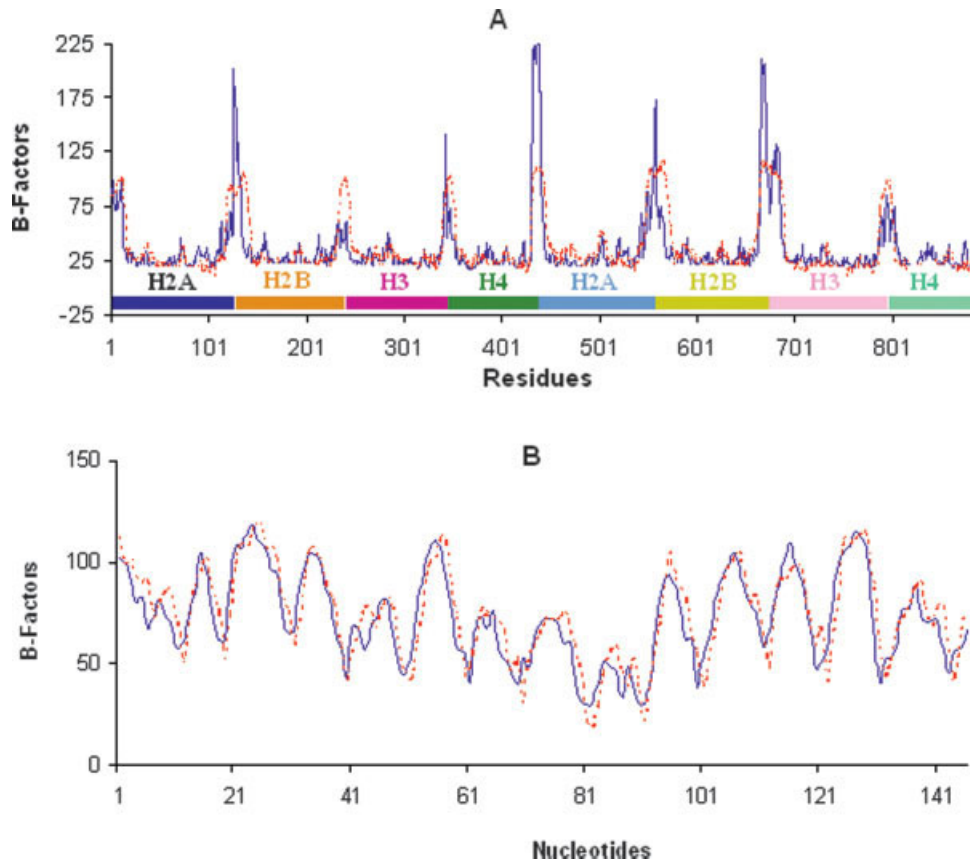


Fig. 4. Comparison of theoretical (continuous curves) and experimental (dotted curve) B-factors, illustrated for the nucleosome 1EQZ. (A) Thermal fluctuations of amino acid in the histone octameric core. (B) B-factors corresponding to DNA nucleotides.

tetramer and those between the 2 H2A.Z–H2B dimers, which induce local perturbations in the structure near the interfaces between the dimers and central tetramer.

The NMA of the global dynamics of nucleosome has been performed using the EN models. Fluctuation amplitudes are predicted using either the GNM or ANM, while the determination of fluctuation vectors requires the use of the ANM.²⁹ The GNM has the advantage of being one order of magnitude faster, and is resorted to unless the directionalities of the motions are explored. The structures 1F66 and 1EQZ differ in their lengths (see above). The dynamics of common residues have been compared. The Kirchhoff matrix of inter-residue contacts is constructed using the C α atoms for representing the amino acids, and the P and O4* atoms for representing the DNA nucleotides. Cutoff distances of 10 Å, 15 Å, and 18 Å have been adopted for protein–protein, protein–DNA, and DNA–DNA interactions, respectively. Molecular graphics images were produced using the UCSF Chimera package from the UCSF Computer Graphics Laboratory.⁴⁷

RESULTS AND DISCUSSION

For a better understanding of the nucleosome dynamics, a 2-step analysis has been performed. First, we examine the overall dynamics of the nucleosome. Two essential quantities, the mean-square fluctuations of residues and their cross-correlations, are analyzed and compared with experimental data. Second, we proceed to a more detailed analysis by dissecting the overall dynamics into the contributions of individual modes of motions, and focusing on the slowest (or global) modes that dominate the observed behavior. The global mode shapes of each histone monomer in the context of the octameric, DNA-bound structure are analyzed to identify the rigid and mobile parts of the structure, as well as the dominant mechanisms of motion and the type of couplings between the cooperative motions of different structural elements. Major differences in the collective dynamics of the nucleosome with ordinary histones and the nucleosome with histone variants are elucidated.

Thermal Fluctuations of the Nucleosome

Figure 4 compares the experimental (from X-ray crystallographic studies; dotted curves) and presently computed (from EN analysis; continuous curves) B-factors. Figure 4(A) displays the B-factors corresponding to the α -carbons of octameric histones as a function of residues index. The curves also reflect the distribution of the mean-square (ms) fluctuations of individual residues in the folded state, as the B-factors (B_i) scale with the ms fluctuations, $\langle(\Delta R_i)^2\rangle$, in the equilibrium positions, as $B_i = (8\pi^2/3) \langle(\Delta R_i)^2\rangle$ for residue i .

Figure 4(B) describes the B-factors of the P atoms of one of the 2 DNA strands. The periodicity of the curves reflects the different mobilities of the solvent- and protein-exposed segments of the helical turns, with solvent-exposed regions enjoying higher mobility. The agreement between theory and experiment is excellent and supports the use of the present approach for further analysis of nucleosome dynamics.

Cooperative Inter- and Intradomain Motions of the Handshake Dimers

Figure 5 shows the maps that describe the correlations between the motions of residues within the dimers H3-H4 and the dimers H2A (H2A.Z in 1F66 and H2A.1 in 1KX4)-H2B (H2B.2 in 1KX4) for the 3 examined structures, labeled 1–3. The schematic representations of the secondary structures of the monomers (colored according to Figs. 1 and 2) are shown on the left and right ordinates and the abscissa. Each map essentially consists of 4 blocks, 2 along the diagonal, and 2 off-diagonal. Those along the diagonal reveal the autocorrelations of residues within the individual histone chains, while the off-diagonal blocks refer to the cross-correlations (or intermolecular interactions) between the monomers of the indicated dimers. The uncorrelated regions are colored purple and the inner regions colored green represent the correlated regions, with the degree of coupling increasing toward the diagonal or inner contours. The regions shown by light gray shades indicate the anticorrelated domains, and the cyan regions correspond to the most strongly anticorrelated regions. The anticorrelated regions are coupled, move in concert, but in *opposite* directions, whereas the correlated pairs undergo concerted fluctuations in the *same* direction. Uncorrelated regions are either decoupled or undergo motions perpendicular to each other.

The correlation map for the dimer H3-H4 reveals that the loops L1 and L2 of H3 are involved in anticorrelated motions with respect to each other. The motions of the short helices $\alpha 1$ and $\alpha 3$ in H3 are correlated with the neighboring loops L1 and L2, respectively, while the central long $\alpha 2$ helix is divided between these 2 blocks, consistent with a global hinge bending near its center. Within H4, the residues from N-terminus to the central residues of the helix $\alpha 2$, and the rest of the residues define two highly anticorrelated domains.

With the observed correlated, as well as anticorrelated, domain motions across the monomers H3 and H4, it is clear that the region formed by loop L2 and adjoining short helix $\alpha 3$ of H3, and loop L1 and the preceding short helix $\alpha 1$ of H4 form a highly correlated block. Likewise, L1 and $\alpha 1$ of H3 and L2, and $\alpha 3$ of H4 form a second block moving in concert. The 2 blocks move in opposite directions. The second block also includes the N-terminus of H4 that contains the gene silencing residues,⁴⁸ revealing the dynamic coupling of this functional region to the $\alpha 1$ helix of H3. The long helices $\alpha 2$ of both histones apparently bent near a central residue, L104 in H3 and H76 in H4, which act as hinge centers coordinating the anticorrelated motions of the 2 blocks. The N-terminus of H3 is observed to be very strongly anticorrelated with helices $\alpha 2$ and $\alpha 3$ of H4.

The H3-H4 maps corresponding to the nucleosomes containing histone variants [middle and lower maps in Fig. 5(A)] exhibit in general the same features as those of the nucleosome with ordinary histones (upper), apart from a weakening in the strength of correlations. The above-mentioned highly correlated blocks of the dimer H3-H4 appear to be less coherent in general, as do the cross-

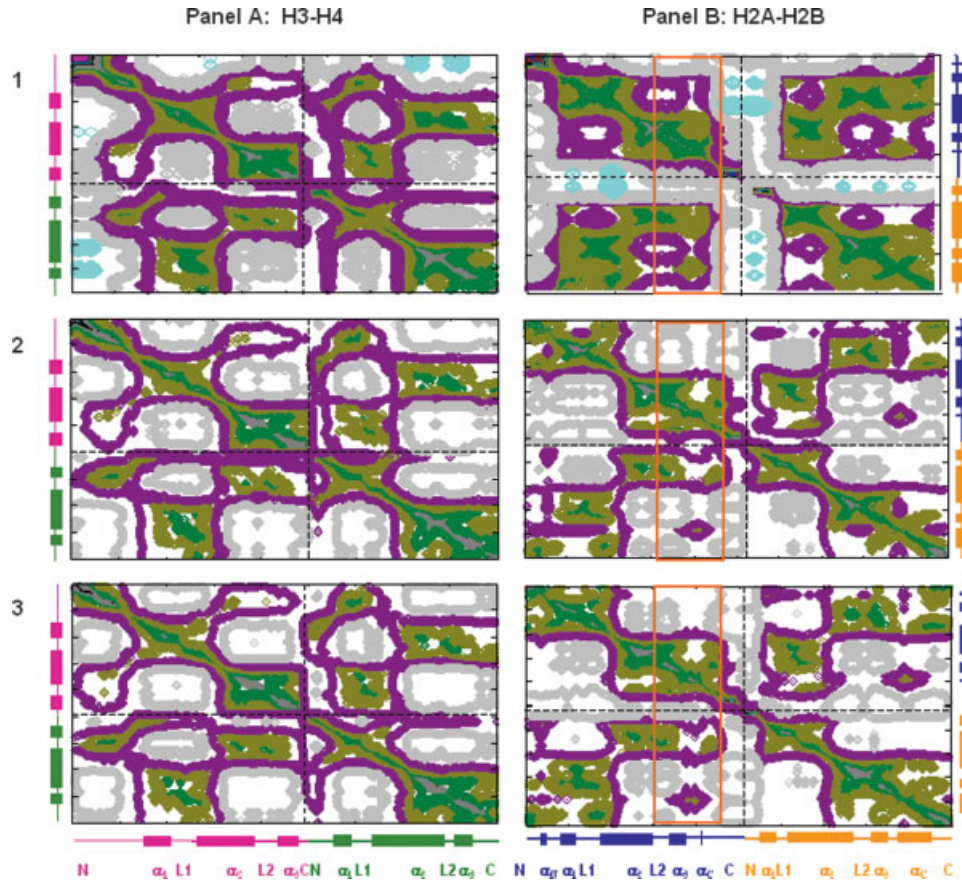


Fig. 5. Cross-correlations between the motions of residues of dimers H3-H4 and H2A-H2B in 1EQZ (1), 1F66 (2), and 1KX4 (3) crystal structures. The uncorrelated residues (colored purple) separate the correlated (where amplitude increases from light green, dark green, and dark gray) and anticorrelated domain (colored gray) regions.

correlations across the monomers. We note in particular the disappearance of the anticorrelations between the H3 N-terminus and the H4 α_2 and α_3 . The introduction of H2A and H2B variants thus affects the global dynamics of the entire nucleosome.

The upper right map in Figure 5(B) reveals that the dimer H2A-H2B of ordinary nucleosome exists as a highly inter- as well as intracoupled dimer. Almost the entire monomers H2A and H2B are engaged in correlated motions, except for the C-terminal segment of H2A and the N-terminal helix N α of H2B. We note that the C-terminus of H2A inserts into the H3-H4 dimer, which may explain its decoupling from the rest of the H2A-H2B dimer. Likewise, the N-terminus of H2B was invisible in the 1EQZ X-ray structure, in accord with its decoupling from the collective dynamics of the dimer. In the H2A.Z variant, the coherent domain motions that exist within the H2A histone are highly disrupted, and the residues that are uncorrelated in H2A become anticorrelated.

The comparison of the maps 1 and 2 in Figure 5(B) indicates that significant differences in intra- and intermolecular correlations exist between the major H2A and the variant H2A.Z. In particular, the H2A.Z residues Arg81-Lys119 located at the interface between the (H3-H4)₂

tetramer and the (H2A-H2B) dimer exhibit substantial decreases in their couplings to the helix-loop α_1 L1 on the same monomer (H2A.Z), and to the loop-helix L2 α_3 on the neighboring (H2B) monomer (see the portions of the map enclosed in the orange boxes). The loss of these long-range correlations implies an inefficient propagation of motion, or communication, between the nucleosome core regions near the central tetramer, and those adjoining the wrapped DNA. This loss in communication, or cooperativity, is in accord with the experimentally observed chromatin-destabilizing role of H2A.Z.¹⁵ The “destabilization” of the chromatin function is thus attributed, according to this analysis, to the disruption of the correlated, or concerted, changes in nucleosome conformation. The histone H2B also exhibits inter- and intracorrelated domain motions, the cooperative nature of which is highly dependent on H2A mobility, with the cooperativity of the motions decreasing with enhanced mobility of the H2A.Z.

In general, the correlations between the motions of the chains H3 and H4 are quite similar in the 3 structures, whereas in H2A.Z-H2B, H2A.1-H2B.2, and H2A-H2B dimers, different patterns of domain interactions are observed. In H2A-H2B dimer, both monomers are involved in highly concerted/cooperative intramolecular motions, as

well as intermolecular interactions with their counterpart monomer. That may be one reason for observing larger conserved domains in H2A-H2B dimer. On the other hand, in the dimers H2A.Z-H2B and H2A.1-H2B.2, the inter- and intramolecular correlations are weakened. The weaker couplings between the monomers are manifested by the higher amplitude motions (see Fig. 6) in the variants compared to their counterparts in the ordinary nucleosome. Such changes in inter- as well as intramolecular domain correlations might shed light into the distinctive transcriptional activity of the nucleosome with variant histone monomers.

Global Mode Shapes of the Handshake Motifs

The behavior illustrated in Figures 4 and 5 reflects the result from an ensemble of normal modes. Next, we proceed to a closer examination of the 2 lowest frequency modes, shortly referred to as modes 1 and 2. The slowest modes usually involve the entire structure and are thereby referred to as global modes. They contribute to the observed spectrum of motions scales with their inverse frequencies (or corresponding eigenvalue of the Kirchhoff matrix). A small subset of slow modes usually dominates the overall dynamics, and the slowest 1 to 2 among them have been shown in numerous studies to drive motions relevant to biological function.^{33–43}

Figure 6 illustrates the global mode dynamics of the monomeric histones, computed for 1EQZ (blue curves), 1F66 (red), and 1KX4 (green). The results are displayed for one set of monomers (labeled as H3, H4, H2A, and H2B), with the global dynamics of the corresponding second monomers (copies) being almost identical. The ordinate represents the distributions of the square displacements of individual residues induced by the first (solid curves) and second (dotted curves) modes. The secondary structures of the monomers (colored according to Figs. 1 and 2) are shown along the abscissa. The histone–DNA interacting sites, L1, L2, and $\alpha 1$, are indicated, along with a few other interacting sites of interest (e.g., minima serving as global hinge sites). It is interesting to observe that (1) the nucleosomes with the variant histones (red and green curves) generally exhibit larger amplitude of motions compared to the nucleosome with ordinary histone monomers, and (2) the residues that are dynamic in one mode behave as rigid domains in the other mode, and vice versa.

In the first mode, the residues Arg24-Ile30 of H4 (i.e., residues 1–7 in Fig. 6), which are involved in gene silencing, exhibit relatively high mobility, which is consistent with their active participation in functional dynamics.⁴⁸ In the H2A monomer, the peak observed in the first mode corresponds to its dynamic L2 loop (Leu77), which interacts with the dynamic loop L1 of H2B. We note in particular that the residues Lys79 in loop L2 of H2A and Ser53 in loop L1 of H2B that interact with the minor groove of DNA are highly dynamic. The regions L2 of H2A.Z, L1 of H2B, and $\alpha 1$ of H3 of each monomer exhibit higher amplitude motions in the variant nucleosome. It has been determined that in the ordinary nucleosome,

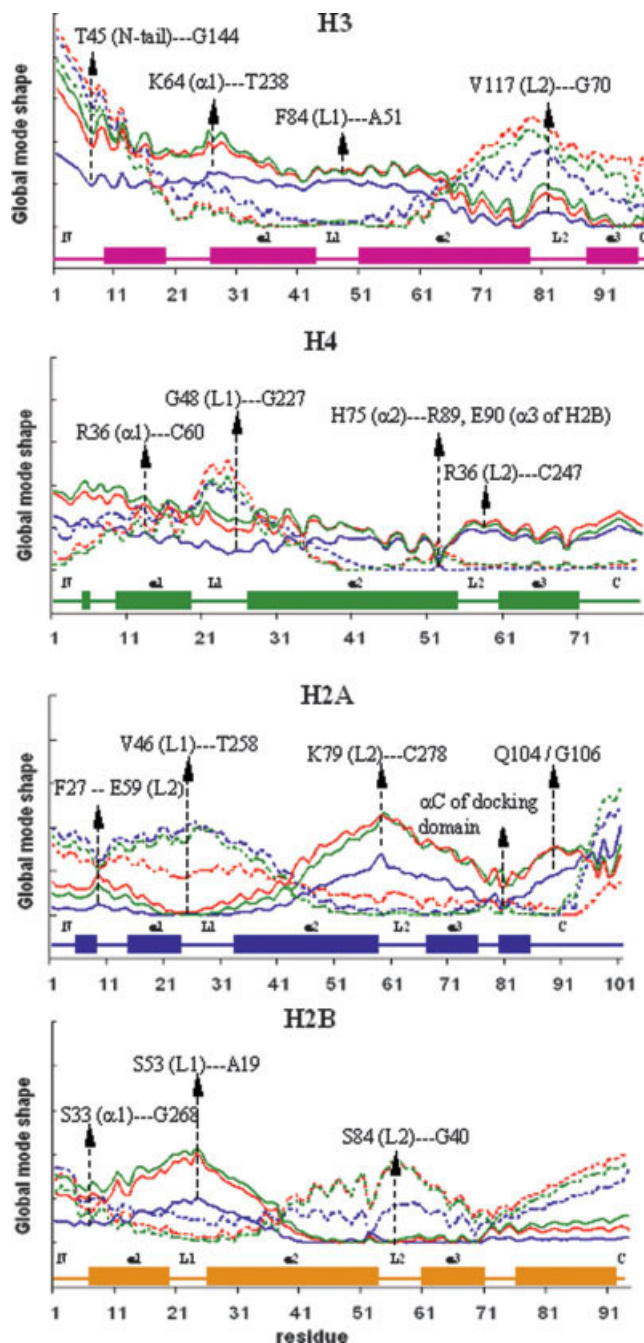


Fig. 6. Comparison of the global mode shapes of monomeric histones H3, H4, H2A, and H2B computed with the GNM for the crystal structures of the ordinary nucleosome 1EQZ (blue), and 2 nucleosomes with histone variants, 1F66 (red) and 1KX4 (green). The curves scale with the amplitude of motions undergone by different structural elements in mode 1 (solid curves) and mode 2 (dotted curves). Arrows indicate the hydrogen-bonding sites between the amino acid residues and the nucleotides located at the L1, L2, $\alpha 1$, and $\alpha 2$ sites along with other interacting sites of interest (e.g., minima serving as global hinge sites).

these regions form hydrogen bonds with the neighboring DNA nucleotides, which are likely to be perturbed, if not broken, in the variant. However, it should be noted that our model pertains to the changes in α -carbon, and P- and O4*-atoms coordinates, and only the changes in hydrogen

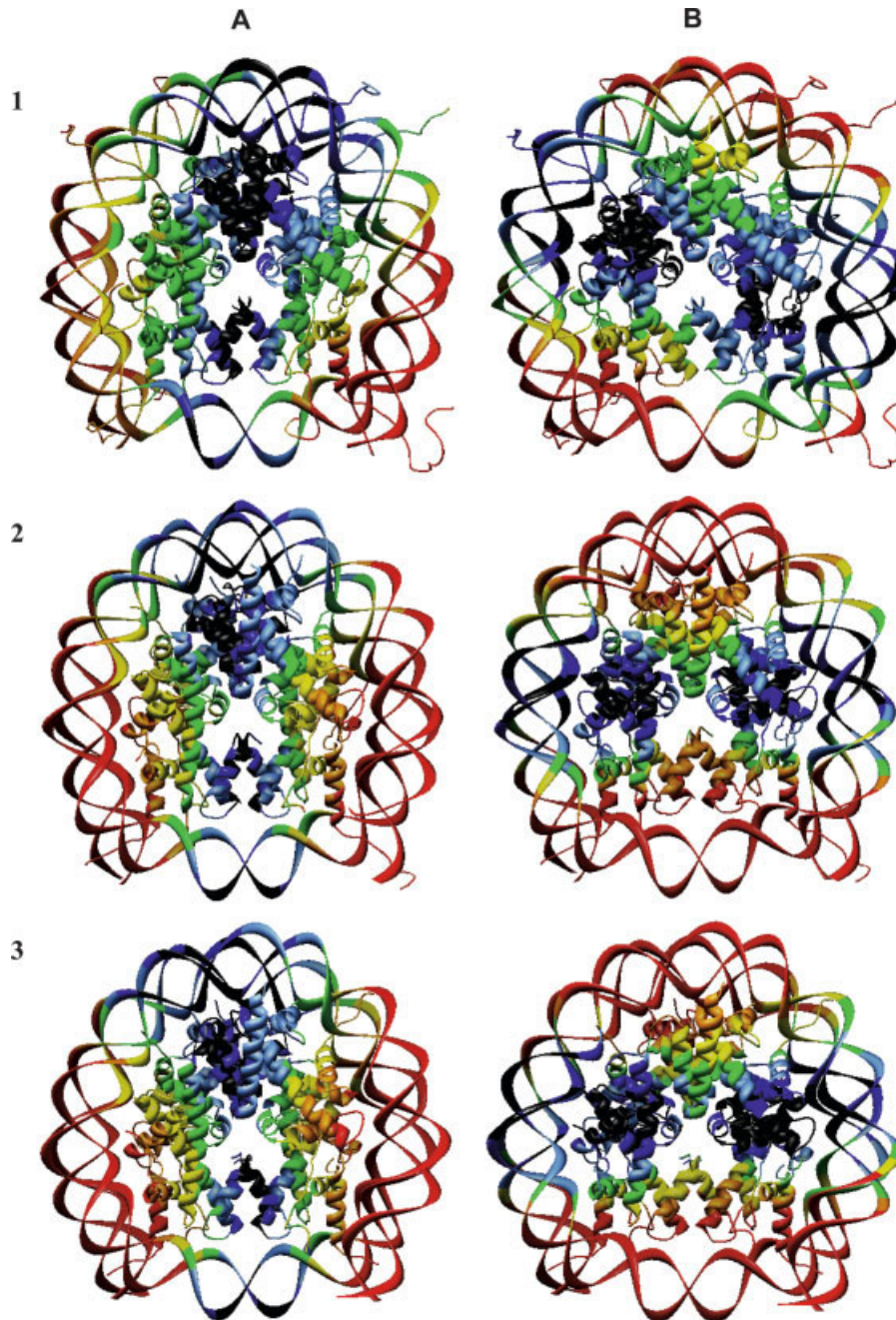


Fig. 7. Color-coded representation of the dynamics of 1EQZ (1), 1F66 (2) and 1KX4 (3) in the first (A) and second (B) collective mode.

bonds that affect these backbone coordinates are taken into consideration in the ANM.

In mode 2, we observe the docking domain of H2A (residues from Ile82 to Ile120, i.e., residues 63–101 in the Fig. 6) to be highly stable (minimal fluctuations) except for the C-terminal region. This region is highly conserved according to the experimental results, and the equivalent region of *Drosophila* H2A.Z is essential in fly development.¹⁸ The hinge domain corresponding to α C helix of the docking domain is indicated in Figure 6.

The complementary shapes of the 2 modes corresponding to the monomers H2A and H2B are noteworthy. These are essentially sinusoidal shapes with a 2-fold symmetric origin at Gly47 (in H2A) and Ser39 (in H2B), the second mode being almost the mirror image of the first. In general, it is observed that the hinge regions observed in one mode behave as highly mobile dynamic regions in the other mode, and vice versa. Overall, a strong cooperativity between the global dynamics of the H2A and H2B monomers is indicated.

Global Dynamics of Nucleosome

Figure 7 shows the dynamics of nucleosomes in a color-coded fashion [from black (rigid) to red (most flexible)] for the first (A) and second (B) slowest modes of structures [1–3]. The histone tails of the 3 nucleosomes vary in length, so the calculations have been performed with all the residues of histone tails, as well as with the common histone tail residues. Both observations of nucleosome dynamics (with full tail domains, as well as with common tail domains) revealed similar pattern of nucleosome dynamics, reported here.

A major observation is the highly symmetrical dynamics of the overall nucleosome with respect to the dyad axis (vertical axis in the present view), consistent with the comparable mobilities of the copies of each histone pointed out above.

In the first mode, the rigid domains fall along the dyad axis of nucleosome. The spatially conserved domains are identified at (1) the H2B residues from L2 through the C terminus, (2) the H2A residues around the loop L1, (3) the residues from helix α_3 to the C-tail of histone H3, and (4) the close neighborhood of His75 on H4 α_2 helix. The N-termini of histones have been experimentally proven to mediate most of the protein–DNA interactions, and their mobilities are essential in the regulation of eukaryotic transcription.⁴⁹ In our study, the N-termini are shown to be highly dynamic in both modes. In particular the highly dynamic N-tail of H3 is engaged in a highly cooperative motion with the neighboring DNA segments. As a result, the wrapped DNA also exhibits a symmetric dynamics with respect to the dyad.

In the second slowest mode [Fig. 7(B)], the dynamics has been identified as conjugate to the first slowest mode of motion; that is, the central region of nucleosome perpendicular to the dyad axis is highly constrained (rigid), while several domains, which were severely almost rigid in mode 1, show significant mobilities. All N-termini of histones except for H4 in the nucleosome with ordinary histones show high mobilities, consistent with the disordered structures of the N-termini of histones.⁵⁰ In the nucleosome, the tetramer (H3-H4)₂ is positioned on both sides of the dyad axis and interacts with one of the DNA strands, and so the dynamics of (H3-H4)₂ affect the dynamics of the particular DNA strand interacting with (H3-H4)₂. Loop L1 and C-terminus in H2A, helix α_2 , and C-terminus in H2B, Loop L2 and N-tail domain in H3, and the H4 L1 loop show the highest mobilities. The most constrained regions that also constrain and control the DNA motions on both sides of the dyad axis are composed of H3 L1, H4 N-tail, α_2 , L2 and α_3 , H2A α_3 , α_C , and adjoining segments (including Q104), and H2B L1 and L2.

The comparison of the dynamics of the ordinary nucleosome (1) with that containing the variants (2 and 3) shows that the direction of the loci of rigid (black) regions changes from a diagonal orientation in (1) to a horizontal one in (2) and (3). Given that the first mode symmetry axis is along the perpendicular axis, the joint contribution of the first 2 modes would then be expected to induce an overall higher and more evenly spread mobility in all

chains of the variants, compared to that in the ordinary nucleosome. Experimental report on the transcriptionally active conformation of nucleosome with the variant H2A.Z,⁸ suggests the perturbed dynamics of (H2A.Z-H2B) dimers and the N-terminus of H3 in physiological conditions.⁵⁰ The second slowest mode could explain the different global dynamics of transcriptionally active nucleosomes, while the first mode is invariably preserved in the 3 structures.

Directions of Global Mode Dynamics of Nucleosome

The nucleosome dynamics were further analyzed using the ANM to identify the directions of nucleosome motions. The histone octamer is a 2-fold symmetric biomolecular complex, and the pseudodyad axis of nucleosome is defined to pass through the center of the nucleosome, so that the C-terminal α_3 helices of H3 and H2A.Z are located very close to this dyad axis (shown in Fig. 1). For easier understanding, the nucleosome dynamics are explained with respect to the dyad axis. The dynamics of 1F66 and 1KX4 are very similar, so we present the results for 1F66 only.

Figure 8 shows the dynamics of nucleosome 1F66 in the first global mode. The crystal structure is shown in gray and the 2 fluctuating conformations predicted by the ANM are shown in magenta and cyan. The latter conformations are generated by adding and subtracting the ANM-predicted deformation vector Δr (corresponding to the global mode of all residues and nucleotides) to–from the crystal structure coordinates. For visual clarity, conformations at different views are displayed and the directions of deformations are shown by arrows. Figure 8(A) illustrates the front view of the nucleosome, and Figure 8(B and C) illustrate the side view along the dyad axis, and the side view perpendicular to the dyad axis, respectively. In the first mode, the regions along the dyad are considerably rigid, while the other 2 sides of nucleosome are fluctuating perpendicularly to the plane of dyad. The whole nucleosome tends to bend with respect to the dyad axis in an out-of-plane fashion. This mode of dynamics supports the experimental evidence of the dissociation of the peripheral regions of DNA from the histone octamer at relatively low ionic strength.⁵¹ The origin of such a bending mechanisms is further dissected by inspecting the dynamics of the dimers of H3-H4 and H2A.Z-H2B.

Figure 8(D and F) illustrates the dynamics of the (H3-H4)₂ and 2(H2A.Z-H2B) tetramers, respectively, from the same perspective as Figure 8(A). Figure 8(E) illustrates the dynamics of (H3-H4)₂ according to Figure 8(B). For clarity, the conformation (cyan) generated by the subtraction of the residue fluctuation vector Δr is not shown. The central portion of the (H3-H4)₂ tetramer is highly stable, while the peripheral regions appear to undergo anticorrelated deformations. On the other hand, the 2 (H2A.Z-H2B) dimers undergo anticorrelated out-of-plane motions with respect to the plane defined by the DNA ring. It is known that transcriptionally active nucleosome is prone to dissociate, and the dissociation is initiated by the release of H2A histones followed by the separation of (H3-H4)₂ tetramer. That is supported by the larger

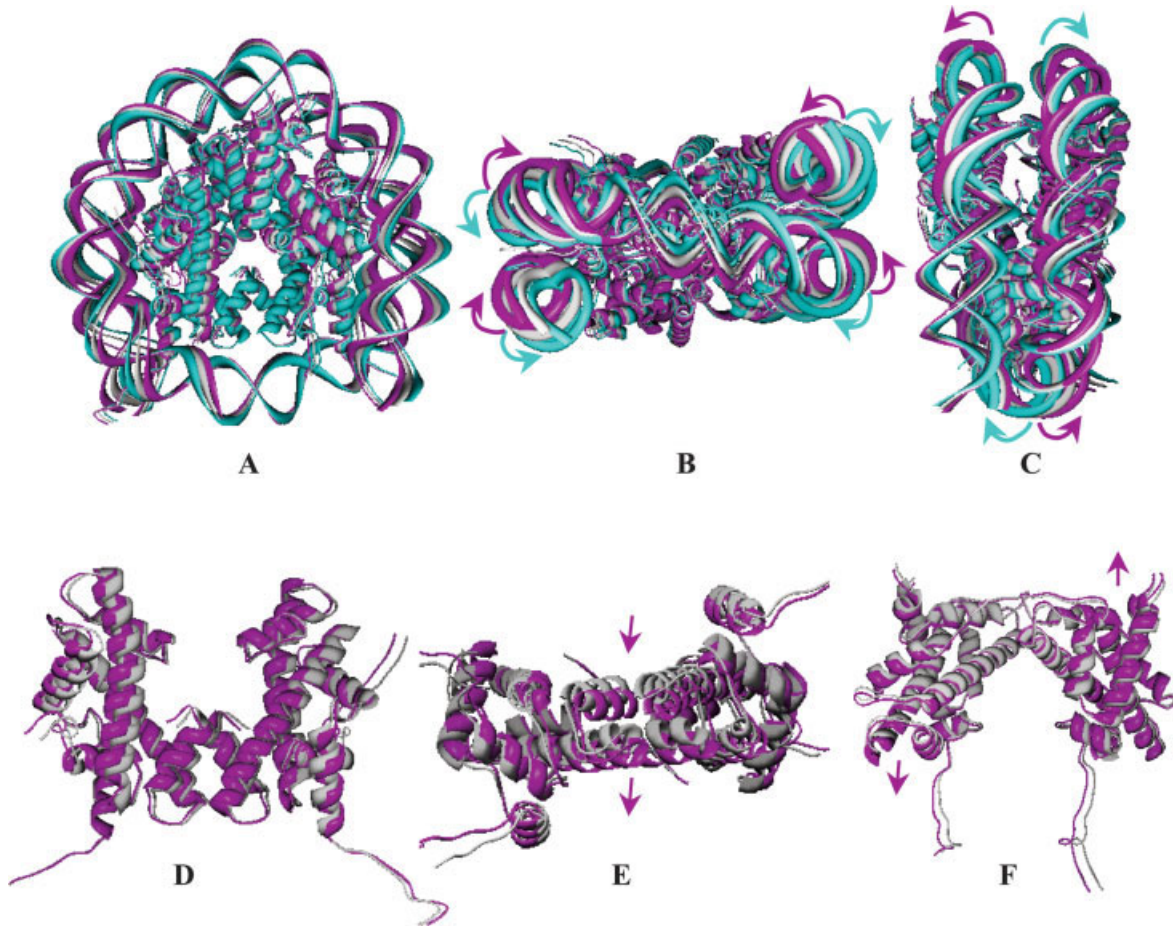


Fig. 8. Superposition of crystal structure and the two deformed conformations of the nucleosome with histone variants 1F66, generated using ANM by adding (magenta) and subtracting (cyan) the residue fluctuation to the crystal structure in mode 1: (A) front view; (B) view along the dyad axis; (C) view perpendicular to the dyad axis. The directions of motion are indicated by arrows. (D and E) The dynamics of $(\text{H3-H4})_2$ according to the front view and along the dyad axis, respectively. (F) $2(\text{H2A.Z-H2B})$ dimers in mode 1.

amplitude of the out-of-plane distortions of the (H2A.Z-H2B) dimer compared to the more restricted in-plane motions of the $(\text{H3-H4})_2$ tetramer core.

In the second slowest mode of 1F66 (Fig. 9), the nucleosome tends to compress and relax with respect to the dyad axis, and the vibrations are constrained to the plane of the ring. Similar to Figure 8, the superposition of the ANM-generated conformations, as well as the crystal structure, is shown in Figure 9(A–C). The arrows along the 3 different views of the nucleosome oscillation in the second slowest mode explain the stretching–compression of the nucleosome in this mode. Figure 9(D and E) explain how the tetramers, $(\text{H3-H4})_2$ and (H2A.Z-H2B) , are involved in the dynamics. In the deformed conformation (colored magenta), loop L1 and the C-terminal $\alpha 3$ helices of H3 monomers are stretched along the dyad axis, and the remaining portions of the $(\text{H3-H4})_2$ tetramer are compressed toward the dyad axis. Similarly, in $2(\text{H2A.Z-H2B})$, the neighboring loops, L1 of H2A.Z and L2 of H2B, are stretched along the dyad axis, and the lateral sides of H2A.Z-H2B dimers are being compressed toward the dyad axis. Altogether, the nucleosome expresses a breathing motion along the dyad axis, with a massive distortion of

nucleosomal DNA, which is brought about mainly by the histone–DNA interaction.⁵¹

Effect of DNA on the Dynamics of Histone Octamer

We analyzed the relative mobilities of the octameric histone core residues in the absence of the wrapping DNA to assess the effect of protein–DNA interactions on the observed dynamics. It is interesting to note that the dynamic of histone octamer without DNA is not as coordinated as observed in the dynamics of the nucleosome. The rigid and dynamic domains of the octameric histone core are not symmetrically distributed either. These observations may be attributed to the regulation of nucleosome by its interaction with DNA and the importance of DNA–protein interactions over the function of nucleosome. Overall, these observations highlight two important features: (1) Attempts to analyze the histone octamer dynamics in the absence of its interaction with the DNA, or that of the DNA in the absence of the histone octamer are likely to miss the functional mechanisms of either component, and (2) the interaction between the histone octamer and the DNA regulates the collective motions of the complex,

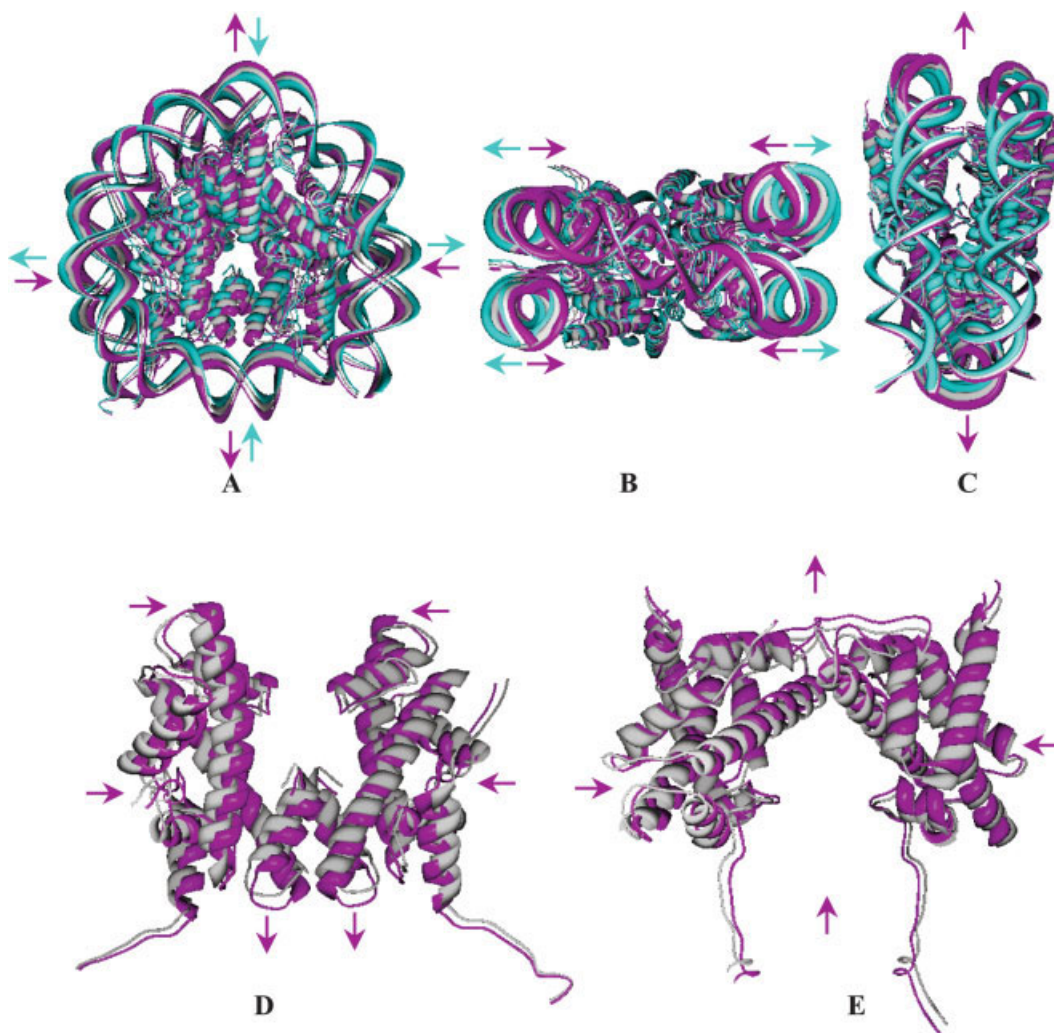


Fig. 9. Superposition of the crystal structure and the 2 fluctuating conformations of 1F66 found by ANM analysis, by adding (magenta) and subtracting (cyan) the residue displacements driven in mode 2: (A) front view; (B) view along the dyad axis; (C) view perpendicular to the dyad axis. The direction of motion is indicated using arrows. (D and E) Dynamics of $(\text{H3-H4})_2$ and $2(\text{H2A.Z-H2B})$ dimers, respectively, in mode 2.

which in the absence of intermolecular interactions are significantly more disordered.

Coordinated Dynamics of Nucleosomal DNA by Histone–DNA Interaction

Figure 10 shows the fluctuations of the DNA nucleotide in the global (first) mode of the ordinary nucleosome (continuous curve) and the nucleosome with the variant histones H2A.Z (dotted curve). Figure 10(A and B) illustrates the 2 strands. The labels indicate the close intermolecular contact regions between the DNA and the indicated histone chains, and structural elements of the nucleosome core. We notice that the DNA in the nucleosome with the variant histone H2A.Z undergoes relatively larger amplitude motions compared to the ordinary nucleosome, consistent with the weakening of intermolecular interactions and correlations in the variant observed above. The most severely constrained nucleotides are those interacting with the nucleosome core elements (1) H2A α 1 and L1, (2)

H2B L2, (3) H3 L1 and L2, and (4) H4 L2. Regions near the histone chains' termini, on the other hand, exhibit relatively high mobilities (peaks in the distributions).

We note that both the above results (first mode), as well as the B-factors presented in the Figure 4(B) (all modes), are obtained with the ANM. The adoption of the ANM is supported by the excellent agreement with experimental data (Fig. 4). The first mode shape computed with the GNM showed some differences from the ANM results, at the position of the base pairs 41 to 51, for example. This type of discrepancy may be attributed to the choice of cutoff distances.^{29,32} In fact, while the optimal cutoff distance for amino acid pairs has been thoroughly tested and confirmed in previous work (to be around 7.0 Å), the optimal values for nucleotides have not yet been established. This and a few recent papers support the adoption of a relatively large (16–18 Å) cutoff distance in order to take account of interstrand couplings in DNA.

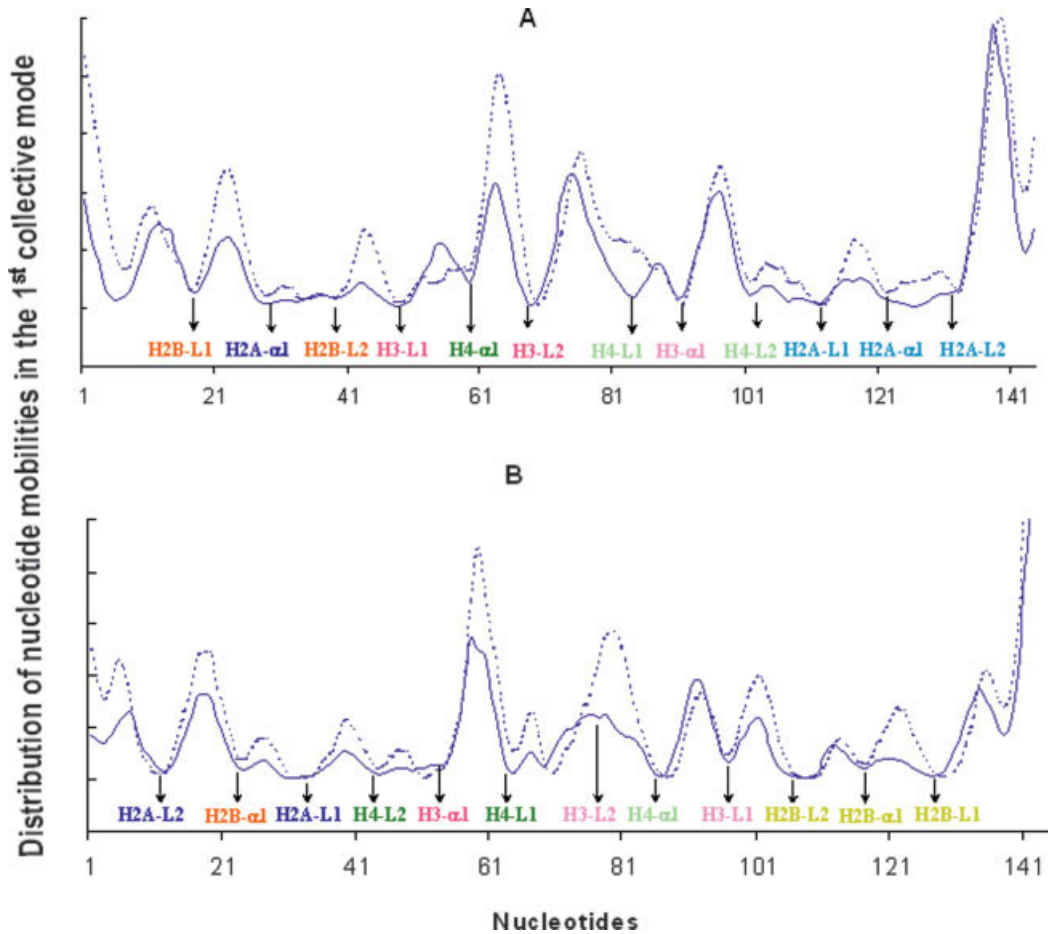


Fig. 10. Comparison of the fluctuations predicted by the ANM for the nucleosome DNA nucleotides. (A and B) Results for the two different strands in 1EQZ (continuous curve) and 1F66 (dotted curve), respectively. The labels indicate the histone chains and secondary structure elements that make intermolecular contacts with the DNA.

TABLE I. Changes in Molecular Dimensions Induced by Dominant Modes

Structures	Dimensions along the Cartesian Axes (Å)						
	X axis		Y axis		Z axis		
	Distance	Difference	Distance	Difference	Distance	Difference	
Crystal	103.0		106.2		68.1		
1EQZ	Mode 1+	103.3	0.3	106.2	0.0	68.3	0.2
	Mode 1-	104.3	1.3	106.1	-0.1	67.9	-0.2
	Mode 2+	103.0	0.0	106.4	0.2	67.9	-0.2
	Mode 2-	103.1	0.1	105.9	-0.3	68.3	0.2
Crystal	103.1		106.7		67.6		
1F66	Mode 1+	103.8	0.7	107.9	1.2	68.6	2.0
	Mode 1-	107.4	4.3	105.4	-1.3	66.5	-1.1
	Mode 2+	104.3	1.2	108.4	1.7	67.2	-0.4
	Mode 2-	104.3	1.2	105.0	-1.7	68.0	0.4

Changes in the Volume Over the Normal Mode Dynamics

Table I lists the molecular dimensions along the 3 principal axes (X , Y , and Z) of the structure, and the deformations in these molecular dimensions induced by the first two slowest modes. The Y axis coincides with the

dyadic axis (shown by the vertical arrow in Fig. 1), the X axis is the in-plane perpendicular axis, and the Z axis is the out-of-plane axis that completes the right-handed reference frame. The dimensions of the nucleosome along these principal axes have been calculated using the Insight II package. The changes in the dimensions have been

estimated by adding and subtracting the fluctuations predicted by the two slowest ANM modes to the crystal structure coordinates (used as a reference). The differences in the molecular dimensions along the 3 axes provide a measure of the voluminous changes induced by the global normal modes. Modes 1+ and 1- refer to the deformed conformations associated with mode 1, and modes 2+ and 2- refer to mode 2.

We note that the deformations observed in the variant histones are generally higher than those occurring in the nucleosome of ordinary histones, consistent with the higher mobility of the variants. Notably, an expansion of 4.3 Å is induced by mode 1 perpendicular to the dyad axis, accompanied by compressions of 1.3 Å along the *X* axis, followed by an out-of-plane expansion of 2.0 Å that is accommodated by 0.7 Å and 1.2 Å stretchings along the 2 radial directions. Overall, the result is a bending (or flipping) motion around the dyadic axis accompanied by an expansion along the *X* axis, as illustrated in Figure 8. Mode 2, on the other hand, is essentially manifested by in-plane stretching-contraction (of 1.7 Å) along the dyad axis, accompanied by small (0.4 Å) compression-expansion along the *Z* direction.

CONCLUSIONS

Global dynamics of nucleosomes with native and variant histones revealed the relaxation of nucleosome with several conformations during the dynamics. The most probable mechanisms of motions predicted by the present analysis are (1) the flip (or bending) of both the sides of the nucleosome in an out-of-plane fashion with respect to the dyad axis, accompanied by an expansion along the in-plane (*X*) axis perpendicular to the dyad axis (mode 1; Fig. 8), and (2) the in-plane stretching-compression of nucleosome core resulting in the deformation of the circularly supercoiled DNA (mode 2; Fig. 9).

In the flipping motion of nucleosome, the N-termini of the H3 and H4 histones are highly mobile, consistent with the functional role of these N-tails experimentally observed under physiological conditions.⁵⁰ Other regions distinguished by their high mobility and closely interacting with the wrapped DNA superhelix are the H2A L2 (peak at K79), H2B L1 (peak at S53; Fig. 6). The most severely constrained regions are, on the other hand, the central long helices in H3 and H4, and the respective loops L1 and L2 of H2A and H2B monomers. These latter sites play a critical role in coordinating the collective mode 1.

In the stretching-compression mode, the nucleosome exhibits a breathing motion along the dyad axis, with a massive distortion of nucleosomal DNA, which is brought about mainly by the histone-DNA interaction.⁵¹ Elements exhibiting the highest mobilities in this mode are the N-terminal tail and loop L2 of H3, H4 L1, H2A L1, H2B L1, and the C-tails of H2A and H2B, while the most constrained regions include H3 L1, H4 L2, H2A L2, and H2B L1.

The nucleosomes containing histone variants are found to be significantly more mobile than the ordinary nucleosome. They exhibit weaker intramolecular and intermolecu-

lar couplings/correlations resulting in more disordered or less coherent motions consistent with their higher flexibility. A region exhibiting distinctive dynamics in the histone variants is the helix α C of H2A, known to be the docking region of H2A.Z. While this region is severely constrained and participating in the global hinge center in mode 1 of the ordinary nucleosome, it becomes significantly more flexible in the nucleosome containing histone variants, consistent with the possible weakening of intra- and intermolecular couplings in the variant. The predicted higher mobility/disorder of the variants may facilitate the disruption of the nucleosome. A recent article by Luger and coworkers⁵² described the variant H2A.Z histone as essential for the nucleosome stability at higher ionic strength, which is in disagreement with the earlier studies of Abbott et al.¹⁵ They attributed these discrepancies to the differences in experimental conditions/preparations. However, the present study focuses on the structural dynamics of nucleosome irrespective of ionic strength dependence.

The coupling between the histone octamer and the surrounding DNA superhelix is instrumental in regulating the dynamics of the octamer, and conversely, the closely interacting proteins significantly alter the dynamics of the DNA, signaling the important role of the complexation with histones in regulating the transcriptional activity.

REFERENCES

1. van Holde KE. Chromatin. New York: Springer; 1989. 497 p.
2. Wolffe A. Chromatin: structure and function. San Diego: Academic Press; 1998. 447 p.
3. Ramakrishnan V. Histone structure and the organization of nucleosome. *Ann Rev Biophys Biomol Struct* 1997;26:83-112.
4. Workman JL, Kingston RE. Alteration of nucleosome structure as a mechanism of transcriptional regulation. *Ann Rev Biophys Biomol Struct* 1998;67:545-579.
5. Luger K, Mader AW, Richmond RK, Sargent DF, Richmond TJ. Crystal structure of the nucleosome core particle at 2.8 Å resolution. *Nature* 1997;389:251-260.
6. Richmond TJ, Finch JT, Rushton B, Rhodes D, Klug A. Structure of the nucleosome core particle at 7 Å resolution. *Nature* 1984;311:532-537.
7. Arents G, Burlingame RW, Wang BC, Love WE, Moudrianakis EN. The nucleosomal core histone octamer at 3.1 Å resolution: a tripartite protein assembly and a left-handed super helix. *Proc Natl Acad Sci USA* 1991;88:10148-10152.
8. Suto RK, Clarkson MJ, Tremethick DJ, Luger K. Crystal structure of a nucleosome core particle containing the variant histone H2A.Z. *Nat Struct Biol* 2000;7:1121-1124.
9. Eickbush TH, Moudrianakis EN. The histone core complex: An octamer assembled by two sets of protein-protein interactions. *Biochem* 1978;17:4955-4964.
10. Hayes JJ, Clark DJ, Wolffe AP. Histone contributions to the structure of DNA in the nucleosome. *Proc Natl Acad Sci USA* 1991;88:6829-6833.
11. Hayes JJ, Tullius TD, Wolffe AP. The structure of DNA in a nucleosome. *Proc Natl Acad Sci USA* 1990;87:7405-7409.
12. Davie JR. Covalent modifications of histones: expression from chromatin templates. *Curr Opin Genet Dev* 1998;8:173-178.
13. Brown DT. Histone variants: are they functionally heterogeneous? *Genome Biol* 2001;2: reviews 0006.1-reviews 0006.6.
14. Adam M, Robert F, Larochelle M, Gaudreau L. H2A.Z is required for global chromatin integrity and for recruitment of RNA polymerase II under specific conditions. *Mol Cell Biol* 2001;21:6270-6279.
15. Abbott DW, Ivanova VS, Wang X, Bonner WM, Ausio J. Characterization of the stability and folding of H2A.Z chromatin particles:

- implications for transcriptional activation. *J Biol Chem* 2001;276:41945–41949.
16. Fan JY, Gordon F, Luger K, Hansen JC, Tremethick DJ. The essential histone variant H2A.Z regulates the equilibrium between different chromatin conformational states. *Nat Struct Biol* 2002;9:172–176.
 17. Jackson JD, Gorovsky MA. Histone H2A.Z has a conserved function that is distinct from that of the major H2A sequence variants. *Nucleic Acid Res* 2000;28:3811–3816.
 18. Clarkson MJ, Wells JRE, Gibson F, Saint R, Tremethick DJ. Regions of variant histone His2AvD required for *Drosophila* development. *Nature* 1999;399:694–697.
 19. Santisteban MS, Kalashnikova T, Smith MM. Histone H2A.Z regulates transcription and is partially redundant with nucleosome remodeling complexes. *Cell* 2000;103:411–422.
 20. Cornell WD, Cieplak P, Bayly CI, Gould IR, Merz KM Jr., Ferguson DM, Spellmeyer DC, Fox T, Caldwell JW, Kollman PA. A second generation force field for the simulation of proteins, nucleic acids and organic molecules. *J Am Chem Soc* 1995;117:5179–5197.
 21. Dauber-Osguthorpe P, Roberts VA, Osguthorpe DJ, Wolff J, Genest M, Hagler AT. Structure and energetics of ligand binding to proteins: *E. coli* dihydrofolate reductase-trimethoprim, a drug-receptor system. *Proteins* 1988;4:31–47.
 22. Levitt M, Sander C, Stern PS. Protein normal-mode dynamics: trypsin inhibitor, crambin, ribonuclease and lysozyme. *J Mol Biol* 1985;181:423–447.
 23. Gibrat JF, Go N. Normal mode analysis of human lysozyme: study of the relative motion of the two domains and characterization of the harmonic motion. *Proteins* 1990;8:258–279.
 24. Tirion MM. Large amplitude elastic motions in proteins from a single-parameter, atomic analysis. *Phys Rev Lett* 1996;77:1905–1908.
 25. Bahar I, Atilgan AR, Erman B. Direct evaluation of thermal fluctuations in proteins using a single-parameter harmonic potential. *Fold Des* 1997;2:173–181.
 26. Haliloglu T, Bahar I, Erman B. Gaussian dynamics of folded proteins. *Phys Rev Lett* 1997;79:3090–3093.
 27. Hinsen K. Analysis of domain motions by approximate normal mode calculations. *Proteins* 1998;33:417–429.
 28. Tama F, Sanejouand Y.-H. Conformational change of proteins arising from normal mode calculations. *Protein Eng* 2001;14:1–6.
 29. Atilgan AR, Durrell SR, Jernigan RL, Demirel MC, Keskin O, Bahar I. Anisotropy of fluctuation dynamics of proteins with an elastic network model. *Biophys J* 2001;80:505–515.
 30. Bahar I, Wallqvist A, Covell DG, Jernigan RL. Correlation between native-state hydrogen exchange and cooperative residue fluctuations from a simple model. *Biochemistry* 1998;37:1067–1075.
 31. Haliloglu T, Bahar I. Structure-based analysis of protein dynamics: comparison of theoretical results for hen lysozyme with X-ray diffraction and NMR relaxation data. *Proteins* 1999;37:654–667.
 32. Kundu S, Melton JS, Sorensen DC, Phillips GN Jr. Dynamics of proteins in crystals: comparison of experiment with simple models. *Biophys J* 2002;83:723–732.
 33. Ming D, Kong Y, Lambert MA, Huang Z, Ma J. How to describe protein motion without amino acid sequence and atomic coordinates. *Proc Natl Acad Sci USA* 2002;99:8620–8625.
 34. Tama F, Wriggers W, Brooks CL III. Exploring global distortions of biological macromolecules and assemblies from low-resolution structural information and continuum elastic network theory. *J Mol Biol* 2002;321:297–305.
 35. Tama F, Valle M, Frank J, Brooks CL III. Dynamic reorganization of the functionally active ribosome explored by normal mode analysis and cryo-electron microscopy. *Proc Natl Acad Sci USA* 2003;100:9319–9323.
 36. Bahar I, Jernigan RL. Vibrational dynamics of transfer RNAs: comparison of the free and synthetase-bound forms. *J Mol Biol* 1998;281:871–884.
 37. Bahar I, Erman B, Jernigan RL, Atilgan AR, Covell DG. Collective motions in HIV-1 reverse transcriptase: examination of flexibility and enzyme function. *J Mol Biol* 1999;285:1023–1037.
 38. Temiz AN, Bahar I. Inhibitor binding alters the directions of domain motions in HIV-1 reverse transcriptase. *Proteins* 2002;49:61–70.
 39. Bahar I, Atilgan AR, Demirel MC, Erman B. Vibrational dynamics of folded proteins: significance of slow and fast motions in relation to function and stability. *Phys Rev Lett* 1998;80:2733–2736.
 40. Bahar I, Jernigan RL. Cooperative fluctuations and subunit communication in tryptophan synthase. *Biochemistry* 1999;38:3478–3490.
 41. Demirel MC, Atilgan AR, Jernigan RL, Erman B, Bahar I. Identification of kinetically hot residues in proteins. *Protein Sci* 1998;7:2522–2532.
 42. Keskin O, Jernigan RL, Bahar I. Proteins with similar architecture exhibit similar large-scale dynamic behavior. *Biophys J* 2000;78:2093–2106.
 43. Tama F, Wriggers W, Brooks III CL. Exploring global distortions of biological macromolecules and assemblies from low-resolution structural information and elastic network theory. *J Mol Biol* 2002;321:297–305.
 44. Harp JM, Hanson BL, Timm DE, Bunick GJ. Asymmetries in the nucleosome core particle at 2.5 Å resolution. *Acta Crystallogr D Biol Crystallogr* 2000;56:1513–1534.
 45. Davey CA, Sargent DF, Luger K, Maeder AW, Richmond TJ. Solvent mediated interactions in the structure of the nucleosome core particle at 1.9 Å resolution. *J Mol Biol* 2002;319:1097–1113.
 46. Berman HM, Westbrook J, Feng Z, Gilliland G, Bhat TN, Weissig H, Shindyalov IN, Bourne PE. The Protein Data Bank. *Nucleic Acid Res* 2000;28:235–242.
 47. Huang CC, Couch GS, Petterse EF, Ferrin TE. Chimera: An extensible molecular modeling application constructed using standard components. *Pacific Symposium on Biocomputing* 1996;1:724. <http://www.cgl.ucsf.edu/chimera>
 48. Johnson LM, Fisher Adams G, Grunstein M. Identification of a non-basic domain in the histone N-terminus required for repression of the yeast silent mating loci. *EMBO J* 1992;11:2201–2209.
 49. Ebralidse KK, Grachev SA, Mirzabekov AD. A highly basic histone H4 domain bound to the sharply bent region of nucleosomal DNA. *Nature* 1988;331:365–367.
 50. Smith RM, Rill RL. Mobile histone tails in nucleosomes: assignments of mobile segments and investigations of their role in chromatin folding. *J Biol Chem* 1989;264:10574–10581.
 51. Muthurajan UM, Park YJ, Edayathumangalam RS, Suto RK, Chakravarthy S, Dyer PN, Luger K. Structure and dynamics of nucleosomal DNA. *Biopolymers* 2003;68:547–556.
 52. Park YJ, Dyer PN, Tremethick DJ, Luger K. A new fluorescence resonance energy transfer approach demonstrates that the histone variant H2AZ stabilizes the histone octamer within the nucleosome. *J Biol Chem* 2004;279:24274–24282.